land

MDPI

Article

Identifying Potential Urban Greenways by Considering Green Space Exposure Levels and Maximizing Recreational Flows: A Case Study in Beijing's Built-Up Areas

Tao Liu [1], Le Yu [1,2,3,*], Xin Chen [4], Yunmiao Chen [5], Xiaomeng Li [6], Xinyi Liu [1], Yue Cao [5,7], Fan Zhang [8], Chenggang Zhang [9] and Peng Gong [2,10]

1 Department of Earth System Science, Ministry of Education Key Laboratory for Earth System Modeling, Institute for Global Change Studies, Tsinghua University, Beijing 100084, China; liu-xy22@mails.tsinghua.edu.cn (X.L.)
2 Ministry of Education Ecological Field Station for East Asian Migratory Birds, Department of Earth System Science, Tsinghua University, Beijing 100084, China; penggong@hku.hk
3 Department of Earth System Science, Xi'an Institute of Surveying and Mapping Joint Research Center for Next-Generation Smart Mapping, Tsinghua University, Beijing 100084, China
4 Institute of Loess Plateau, Shanxi University, Taiyuan 030006, China; chenxin@sxu.edu.cn
5 Department of Landscape Architecture, School of Architecture, Tsinghua University, Beijing 100084, China; chen-ym21@tsinghua.edu.cn (Y.C.); caoyue@tsinghua.edu.cn (Y.C.)
6 School of Social Work, China Women's University, Beijing 100101, China; 2401004@cwu.edu.cn
7 Institute for National Parks, Tsinghua University, Beijing 100084, China
8 Institute of Remote Sensing and Geographical Information System, School of Earth and Space Sciences, Peking University, Beijing 100871, China; fanzhanggis@pku.edu.cn
9 School of Social Sciences, Tsinghua University, Beijing 100084, China; zcgice@tsinghua.edu.cn
10 Department of Geography, Department of Earth Sciences and Institute for Climate and Carbon Neutrality, The University of Hong Kong, Hong Kong, China
* Correspondence: leyu@tsinghua.edu.cn

Abstract: Urban greenways are pivotal in enriching urban quality and fostering socio-ecological sustainability. Previous studies on urban greenway networks have often overlooked user-based experience efficiency, leading to the underutilization and insufficient translation of cultural services into human well-being. In this study, we introduce a user behavior-driven assessment framework for planning multifunctional urban greenways that connect parks with high green space exposure and maximize recreational mobility. Beijing's built-up urban areas (BBUA) were selected as the case study area. Firstly, we evaluated the green space exposure of 331 parks in BBUA using an integrated "Availability–Accessibility–Adaptability" assessment framework as potential carriers. Then, through spatially explicit workflows and the least-cost path methodology, we leveraged a vast dataset of 70 million public transportation swipe records to optimize the alignment of multifunctional greenways, prioritizing the criterion of maximizing recreational footfalls. The results showed that the potential greenways network spans 1566.36 km in BBUA, encompassing 93.88% of parks and offering six diverse functions. It can serve 34.39–35.92% of bus recreation passengers, with this ratio tending to be higher on weekends. However, we identified obstacle points (non-greenway sections) in the networks based on residents' view perceptions and panoramic street images, primarily located in densely built-up central areas and along southern trunk roads. By addressing these disconnections, the integrity and connectivity of urban greenway networks in BBUA will be improved. Overall, the framework we present can be used to construct greenway networks that maximize the perceived accessibility for bus-based visitors, with valuable implications for sustainable urban planning and regeneration initiatives.

Keywords: greenways; public transportation; green space exposure; street panoramic view; BBUA

check for updates

Citation: Liu, T.; Yu, L.; Chen, X.; Chen, Y.; Li, X.; Liu, X.; Cao, Y.; Zhang, F.; Zhang, C.; Gong, P. Identifying Potential Urban Greenways by Considering Green Space Exposure Levels and Maximizing Recreational Flows: A Case Study in Beijing's Built-Up Areas. *Land* **2024**, *13*, 1793. https://doi.org/10.3390/land13111793

Academic Editor: Jane Southworth

Received: 26 September 2024
Revised: 19 October 2024
Accepted: 29 October 2024
Published: 31 October 2024

Copyright: © 2024 by the authors. Licensee MDPI, Basel, Switzerland. This article is an open access article distributed under the terms and conditions of the Creative Commons Attribution (CC BY) license (https://creativecommons.org/licenses/by/4.0/).

1. Introduction

Cities worldwide are vigorously expanding urban green spaces [1–3]. These spaces, which encompass greenways, parks, urban forests, waterfronts, and open green areas, are essential components of urban systems [4,5]. They offer diverse ecosystem services, such as regulating urban microclimates [6] and mitigating floods [7], providing cooling down services [8], and carbon sequestration [9], thereby contributing to resilient and sponge-like cities [10,11]. Unlike other static green spaces, greenways are a form of linear green infrastructure that connects various types of open space, such as ecological parks and green parks [12]. Greenways also provide numerous socioeconomic benefits, including enhancing physical and mental health [13], reducing household health costs [14], and offering intangible physiological benefits [15]. Scientific and systematic planning of greenways is crucial for fostering sustainable cities and strengthening social pillars.

Currently, a considerable number of theoretical frameworks for greenway systems planning have emerged [16], most of which integrate environmental, geographic, climatic, and socioeconomic data [17,18]. In terms of greenway planning, there are robust frameworks based on questionnaires [19], the analytic hierarchy process (AHP) approach [18], human-based flows [19], and others [20]. Methods for greenways routing include the greenways network preparation program [21], geographic information models [22], the least cumulative resistance model [23], and the multifactor superposition method [5], as well as spatially explicit approaches [24], network analysis method [25], and landscape connectivity for greenways network routing [26].

The integration of big data into greenways identification is gaining increasing traction [18,27]. Leveraging extensive datasets on recreational flows, such as those derived from shared bicycle trajectories [28], taxi movements [29], and mobile signaling data [30], holds immense potential to optimize the delivery of ecosystem cultural services [31,32]. Moreover, social network data sourced from platforms like TikTok and Facebook, showcasing users' green experiences, serve as pivotal indicators for greenways route selection [33].

Furthermore, high-resolution remote sensing imagery at the tree level, encompassing technologies like LiDAR and drone imagery [34], has emerged as a critical input for urban greenway spatial analysis, facilitating point-based evaluation of green space quality [35]. Notably, the adoption of user-generated street-level view imagery has garnered widespread recognition in greenways planning endeavors [36,37]. This imagery provides insights into citizens' firsthand experiences and engagement opportunities within greenways [38]. Indeed, the amalgamation of diverse big data sources has become the prevailing approach in greenways planning, underscoring interdisciplinary methodologies spanning geographic information technology, deep learning algorithms, remote sensing data analytics, and model optimization techniques [39].

China's urbanization and urban sprawl have been unprecedented over the past two decades [40,41]. Fragmentation of urban landscapes [42,43], significant urban heat island effects [44], as well as scarcity and inequality of green space [45], have been widely observed in China's cities. China's greenway planning exhibits certain deficiencies, marked by uneven spatial distribution and low use frequency [46]. To proactively address the knock-on effects of the dissonance between man and nature, the Chinese government has launched ambitious greenways planning policy package (Figure A3). Mature greenway initiatives predominantly thrive on the fringes of urban areas, while rejuvenating green corridors in old urban area remains a pressing need [47]. Furthermore, a prevalent mismatch between populace and greenway spaces underscores the need for an effective strategy to enhancing access efficiency [48]. Methodologically, conventional approaches suffer from insufficient sample sizes, which leads to a high degree of uncertainty when translating greenway planning blueprints into tangible realities [12]. Another challenge lies in the existing framework's neglect of user mobility-based perspectives, resulting in a reduced frequency of visitor access to greenways. This, in turn, exposes individuals to physical and mental health risks [49].

To fill the significant knowledge gap, we present a user-based driven assessment framework for identifying greenway networks. First, using the "3A" (Availability-Accessibility-Adaptability) framework, we evaluated the green space exposure of 331 parks in BBUA. Parks with high exposure levels were selected as carriers of greenway systems. Then, we used spatially explicit traffic information by filtering weekly transportation swipe data containing 70 million samples. We identified high-recreation-frequency routes as key selections for greenways. Note that the definition of urban greenways in this work is limited to systems that connect urban green spaces, distinguishing them from walking trails, waterfront greenways, etc. The functions of park nodes determine the functions of the greenway network, enabling an optimal configuration of multifunctional greenways. This study addresses the following three questions: (1) What is the spatial pattern of green space exposure level in BBUA? (2) How well laid out and multifunctional is the potential greenway network? (3) Where are the obstacle points in the greenway network located?

2. Materials and Methods

2.1. Study Areas

The Beijing's built-up urban area (BBUA), a cutting-edge metropolis in China, spans over 1088 km^2, primarily encompassing Dongcheng, Xicheng, Chaoyang, Haidian, Fengtai, and Shijingshan districts (Figure 1a). This region boasts an exceptionally compact road and metro system for public transportation, coupled with a high level of human activity. As one of China's most densely populated metropolitan areas, the resident population of the study area has skyrocketed from 2.1 million to 10.9 million inhabitants from 2000 to 2020, which has led to higher demands on the urban green space system. The pattern of urban sprawl in the area revolves around ring patterns and encompasses a total of 4209 public transportation lines and 33,664 stations (Figure 1b).

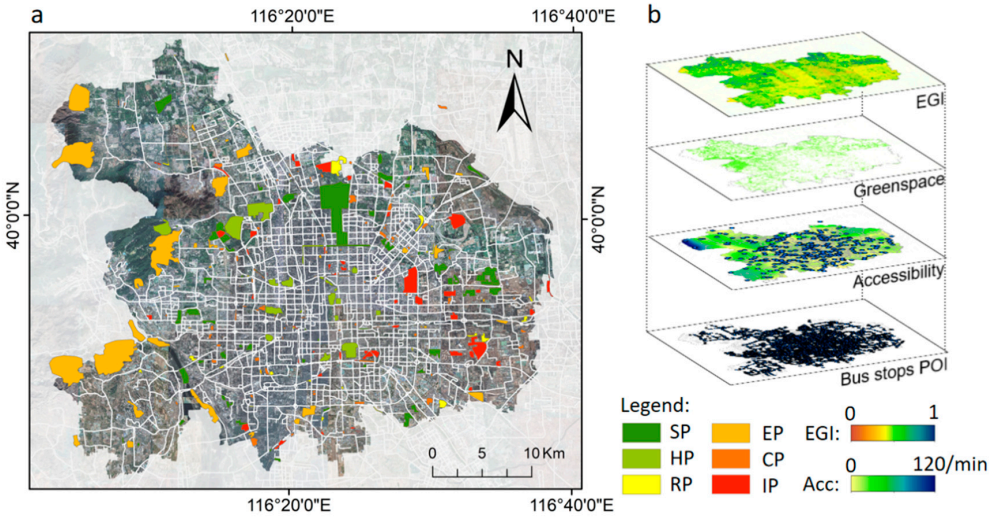


Figure 1. Spatial distribution of roads and parks in BBUA, as well as auxiliary spatial data. (**a**) A spatial map depicting the pattern of roads and parks in BBUA. The white lines indicate roads. (**b**) The diorama map provides supplementary spatially explicit patterns regarding EGI, green spaces, accessibility, and bus stop POIs. **SP:** specialized park; **EP:** ecological park; **HP:** historic park; **CP:** community parks; **RP:** recreational parks; **IP:** integrated parks; **ACC:** accessibility; **EGI:** excess green index).

Nowadays, it is increasingly evident to local residents that they favor greenways. The government has initiated old city renovation projects, whereby low impact buildings are replaced with open spaces such as parks and green areas, aiming to cater to the wishes of the residents and enhancing the sustainability of the city. In our research, we have identified 331 green space-related parks within BBUA, which can be categorized into six distinct types (Figure 1).

2.2. Data Sources and Processing

In this paper, bus traffic and parks area of interest (AOI) data are employed as crucial input variables for this research. Specifically, we captured 4254 point of interest (POI) park data from Gaode Maps (ditu.amap.com), China's authoritative map and navigation sharing platform, by using "park" as the keyword. By eliminating duplicates, removing redundant and irrelevant points, and manually reviewing each one, we initially evaluated 331 POI parks. The actual boundaries of each park AOI were determined by our co-authors using Google Earth tools (earth.google.com). In this work, we only considered green parks with large areas of green space, and excluded non-green vegetation-covered parks such as car parks and basketball parks. By comparing the Beijing Municipal Parks Directory List (https://yllhj.beijing.gov.cn), the 331 parks were categorized into six functions, as shown in Figure 1.

Furthermore, we collected weekly bus traffic data to mine high-volume recreational travel patterns, which contribute to identifying potential urban greenways. All travel data were obtained from the Beijing Public Transport Co. (www.bjbus.com) for the period of February 13th to 19th, 2023 in Beijing, including information on bus stops, times, and trip numbers, among other variables. This dataset integrates transportation cards and quick response code cards from phones, totaling over 70 million card traffic samples. It is essential for analyzing the residents' travel purposes, such as daily commuting, sightseeing, leisure, and shopping. We cleaned the bus data and visualized the bus travel map.

Auxiliary data were gathered to create a geodatabase in support of this work. The Beijing vector street data is available from www.resdc.cn, while the road system used to determine park accessibility was obtained from the OpenStreetMap platform in 2023 (openstreetmap.org). The accessibility network processing involved vector cropping and hierarchical processing implemented on ArcGIS 10.2 (Appendix A for details). We collected precise green space data, with a resolution of 1 m and for the year 2023, from prior research to satisfy the small-scale park requirements (Figure 1). To assess green space quality, we computed each park's excess green index (EGI) via the Google Earth Engine cloud platform and image analysis. All geographic data were projected onto the Krasovsky UTM 50-degree bands. In addition, the acquisition of street view panoramic images was conducted utilizing the street view imagery (SVI) from the Baidu Street View service (Refer to Appendix B). Detailed information can be seen in Table 1.

Table 1. The data list in this work.

Data Lists	Sources	URLs
Big data on bus transport swipe cards	Beijing Public Transport Co.	www.bjbus.com (accessed on 25 September 2024)
Park POI data	Gaode Map Open Platform	https://ditu.amap.com (accessed on 25 September 2024)
Beijing Parks List	Beijing Municipal Forestry and Parks Bureau	https://yllhj.beijing.gov.cn (accessed on 25 September 2024)
Vector boundary of BBUA	Resource and Environment Science and Data Center,	www.resdc.cn (accessed on 25 September 2024)
Google image raster data	a peer-reviewed paper [50] and Google Earth	https://earth.google.com (accessed on 25 September 2024)
Public transport road system	OpenStreetMap	https://openstreetmap.org (accessed on 25 September 2024)
Comments data	Dazhongdianping consumption sharing platform	www.dianping.com (accessed on 25 September 2024)
Street View images	Baidu Street View service	https://api.map.com (accessed on 25 September 2024)

2.3. Methods

To achieve scientifically informed outcomes in planning multifunctional urban greenways network systems, we assessed the human exposure to green spaces of 331 parks as potential greenways carriers using the "3A" framework and mined high-frequency recreational travel routes from transportation swipe data. This work involves four es-

sential steps: (1) assessing park exposure as potential greenway carriers; (2) extracting passenger-based recreation routes from bus transportation data; (3) overlaying each route and identifying high-frequency recreation access routes as greenways; (4) identifying the multifunctional greenways network and obstacle points based on street panoramic image. A visual flowchart is illustrated in Figure 2.

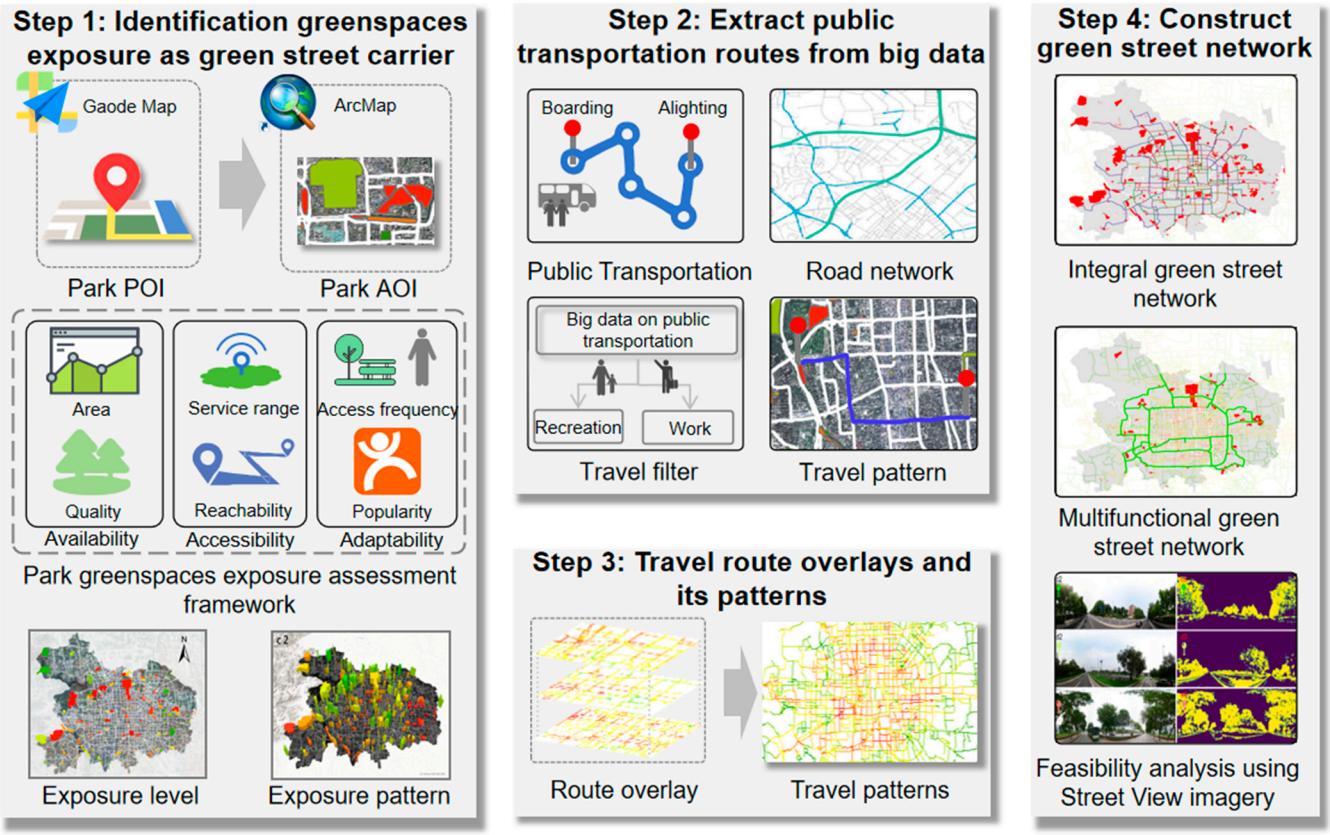


Figure 2. Visualizing technology map.

2.3.1. Park Green Space Exposure Assessment

To assess park green space exposure quantitatively, we adopted the "Availability–Accessibility–Adaptability" (3A) assessment framework, as demonstrated in previous work (Table 2), which provides a convenient and efficient method to evaluate exposure performance in urban green spaces [51]. The "3A" framework can encompass a wide range of dimensions, including natural function potential and human socioeconomic well-being. Identifying the exposure levels in 331 parks is crucial for recognizing park green space carriers, and this framework comprises three primary elements:

Availability: This component illustrates the basic state of green space in parks, encompassing two key indicators: area and quality (Table 2). The green space area is a valuable metric for quantifying green space exposure and is widely used in relevant research. We calculated the green space area of each park using zoning statistical tools in ArcGIS 10.2. Furthermore, we introduced the excess green index (EGI) to demonstrate variations in green space quality (Table 2). For example, the presence of denser vegetation is associated with more robust ecological processes. The EGI is an effective index for monitoring small green spaces such as community parks. To express accurate green space information, high-quality input data of RGB true-color Google remote sensing imagery with 1 m resolution and a time stamp of 2023 were utilized. The exact formula to use is as follows:

$$EGI = 2G - R - B \quad (1)$$

where *EGI* represents the excess green index. *G*, *R*, and *B* represent the green, red, and blue bands, respectively.

Table 2. Park green space exposure assessment system. (We have developed a "3A" framework for assessing the exposure of park's green spaces, which comprises three pillars and six indicators. Below, we provide the proxies for each indicator along with their significance.).

	Systems	Indicators	Agency	Significance
Park green-space exposure	Availability	Area	Green-space area	Larger green areas can increase park capacity and visitor acceptance levels.
		Quality	Excess green index (EGI)	This indicator helps evaluate green space quality; densely vegetated green spaces tend to be more favored.
	Accessibility	Service range	Park type	We quantified the service area of various parks, which is crucial for the surrounding residents.
		Reachability	Transport accessibility	By constructing an OD cost matrix with the road network, we quantified accessibility ranging from 5 to 120 min using Arcmap 10.2 tools.
	Adaptability	Popularity	Popularity of parks	The parks are graded according to their levels in the Beijing Parks Directory, with the high-level parks tending to be more well-known.
		Access frequency	Comments in Dazhongdianping	A greater number of comments reflects higher access frequency, which is essential for human exposure to park green spaces.

Accessibility: We aimed to measure the interaction between humans and the park through two metrics: accessibility and service coverage (Table 2). On the one hand, movement-based human behavior improves access to parks through public transportation. By defining a road network dataset (Table 1), we generated the accessibility radiation area formed by the source points along the topological road network (See Appendix A for details). Using an origin–destination (OD) cost matrix [52], we created a model of the public transportation network with a hierarchy incorporating breakpoints of 5, 10, 15, 30, 60, 90, and 120 min to determine park accessibility (Figure A1). Additionally, we examined the direct and potential impact of various parks on local human perception (Table 2). In accordance with the Chinese standards for park service areas (https://www.mot.gov.cn/), we measured the service areas of various types of parks, which range from 300 m for community parks to 2000 m for comprehensive parks (Table A1).

Adaptability: We then evaluated the impact and popularity of parks on residents (Table 2). The Beijing Municipal Bureau of Landscape Architecture categorizes green parks into four levels, with the highest to lowest levels corresponding to grades A to D. We also considered the frequency and number of parks visits within our framework (Table 2). One challenge we encountered was quantifying visit frequency in small parks. To address this, we utilized an agent-based model based on big data analysis of park evaluations. Specifically, we analyzed the quantity of ratings provided by visitors for each park through Chinese travel mobile apps from Dazhongdianping (Table 1). Parks with higher levels of comments also correspond to higher levels of visits, which is crucial in quantifying residents' exposure to parks. Using the natural segment point method, we categorized exposure levels into five classes, with the two highest exposure classes selected as the carriers for greenways (Figure A6). The "3A" assessment framework for this study is displayed visually below:

We found that the data from the "3A" framework did not follow a normal distribution; instead, it exhibited a heavily skewed left histogram. Parks that are well-known typically exhibit significantly greater amounts of green space and visitor frequency compared to other parks. To address this, we applied Equation (2) to adjust the normal characteristics of the indicator and reduce redundancy in extreme values. Additionally, normalizing the data is necessary to facilitate horizontal comparisons across dimensions [14]. All indicators show positive values, except for accessibility. The normalization formulas are as follow:

$$I_N = ln(j) \tag{2}$$

$$I_{Nj} = \frac{I_N - I_{N_{min}}}{I_{N_{max}} - I_{N_{min}}} \tag{3}$$

$$I_{Nj} = \frac{I_{N_{max}} - I_N}{I_{N_{max}} - I_{N_{min}}} \tag{4}$$

where the datasets matrix was constructed, with rows representing parks (i) and columns representing indicators (j). I_N denotes the normalized values, while I_{ij} represents the values in column j. I_{N_max} and I_{N_min} represent the initial maximum and minimum values of column j, respectively, indicating, the best and worst performance for a certain indicator. I_{Nj} is the new column after normalization. All values were scaled between 0 and 1, where 0 represents the worst and highest performance and 1 represents the highest performance.

2.3.2. Weighting

The indicators were assigned weights to determine their contribution to exposure. To ensure objectivity, we employed the entropy method for weight calculation. A lower information entropy indicates a higher level of information provided by a specific indicator, which is integral to the comprehensive evaluation system. The calculation process is as follows:

$$w_i = \frac{G_i}{\sum_{i=1}^{m} G_i} \tag{5}$$

where w_i is the weight of indicator i, i = 1, 2, 3; m represents the indicator dimension, and $m = 6$ in this work. Gi is the information utility value of indicator i.

$$G_i = 1 - E_i \tag{6}$$

where E_i is the entropy of indicator i.

$$E_i = -k \sum_{j=1}^{n} \sum_{t=1}^{r} P_{ij} \times ln(P_{ij}) \tag{7}$$

where k represents constant and $k = ln\ (m)$. j is the number of evaluation objects, j = . . . 1, 2, 3, n; there are j = 331 in this work. In addition, t is the number of indicators, t = . . . 1, 2, i, r, and $r = 6$. P_{ij} is the proportion of the value of each indicator.

$$P_{ij} = \frac{V_{ij}}{\sum_{t=1}^{r} V_{ij}} \tag{8}$$

where V_{ij} is the standardized value of each indicator.

2.3.3. Identifying Recreation Routes and Potential Urban Greenways

In this paper, the identification of the greenways network relies on the data collected from traffic swipes to spatially determine residents' recreational mobility. The efficiency optimization hypothesis posits that roads with higher numbers and frequency of public passengers for shopping and recreation would benefit more from at-grade greenways. This approach aims to maximize the ecological and aesthetic value of greenways while

enhancing invisible human well-being [2]. Additionally, the greenway community often emphasizes diversity and adaptability in an era of varied requirements. Consequently, greenway systems serving different functions have been established, utilizing six distinct park types and their priority arrangements.

We employed a flow-based process to filter and visualize patterns of passenger traffic flow for recreation and shopping. Specifically, we utilized Arcmap 10.2 software and geographic coordinate information to visualize bus stops and bus route patterns (Figure 3). Typically, work-related passenger trips exceed 8 h for round-trip travel, whereas leisure and shopping trips generally require less than 6 h. Taking this into account, we calculated the time difference from when each sample disembarked from the bus stop to their return to the starting point. Using the decision tree method, we determined the spatial line for leisure and shopping (Figure 3). We excluded some potentially interfering samples and ultimately visualized 400,000 samples (Figure 3).

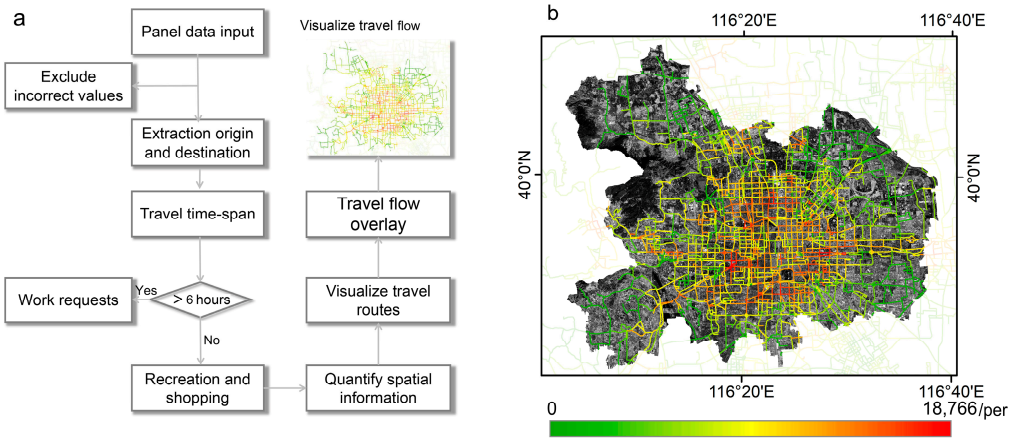


Figure 3. Travel flow extraction and visualization based on big data of bus card. (**a**) Procedure extraction steps. (**b**) Visualizing bus traffic flow map.

Greenways were identified using both qualitative and quantitative methods based on carrier priorities and the high frequency of recreational roads. This plan incorporates only the greenways with the highest pedestrian flow and valuable potential, while also considering the landscape patterns of the surrounding areas. For instance, ribbon parks along roads and waterfront paths will receive prioritization. The least-cost paths (LCP) method is a straightforward and suitable resistance-based modeling approach [53,54]. The quantitative assessment method employs the LCP, where the resistance value in off-road areas is set to converge to infinity, and the resistance value for the bus route is set lower as the passenger flow increases. Additionally, we modified some greenways while adding potentially useful ones that provide valuable ecosystem services, taking into account human requirements, patterns, and maximizing benefits.

2.3.4. Identifying Barrier Points in Greenway Networks

We attempted to use street view images to recognize the barrier points of the greenways network and discuss entry points for improving street greening in BBUA. According to the Baidu development documentation, the API service interface was called, with the field of view parameter set to 360° (fov = 360) [55]. We used Python packages to write a program to retrieve panoramic images, resulting in a total of 3235 images within BBUA. Considering that BBUA is in a temperate monsoon climate, the bare tree trunks in winter can lead to uncertainties in the results. Therefore, only images from March to October were included in the study. In the end, we obtained 1479 Baidu street view images from the last decade.

Here, we considered using the green view index (GVI) to demonstrate the greening performance of roads [56]. The GVI, as an important indicator of spatial greening quality

in urban streets, has been widely used in recent years. Panoramic images are more closely aligned with human perception. The GVI is defined as the ratio of the total green area in street panoramic photos to the total area of the photos. Previous studies have extensively demonstrated the positive effects of high GVI performance on human health and ecological urban development. The GVI, based on multi-angle greening images aligned with human sight-lines, is commonly used to reveal the relationship between green spaces and human health and well-being, and is incorporated into neighborhood environmental audits. We constructed a decision tree to evaluate the green view ratio indicators of street panoramas (Figure A2). In this article, streets with a high GVI are considered greenways within the network, while streets with a low GVI are defined as obstacle points. Overcoming these obstacle points facilitates the creation of a greenways network that is both connected and integrated, contributing to the development of a sustainable urban environment.

3. Results

3.1. The Status of Park Green Space in BBUA

We identified green-related 331 parks AOI, covering a total area of 13,248 ha, equivalent to 9.8% of BBUA (Figure 4). Administratively, Dongcheng boasts the highest number of parks, totaling 108, while Chaoyang has the least with only 18 (Figure A4). In terms of park area, Chaoyang has the largest areas at 4119 ha, while Xicheng only has 352 ha (Figure A4). The percentage difference in park area among the six districts ranges from 7.47% to 10.92%, with Shijingshan deserving particular praise (Figure A4). We observed significant average park size across different districts. Shijingshan district has the largest average park area of 48.38 ha, followed by Chaoyang and Haidian districts with 41.19 ha and 38.72 ha, respectively. Xicheng district has the smallest average park area of 8.38 ha.

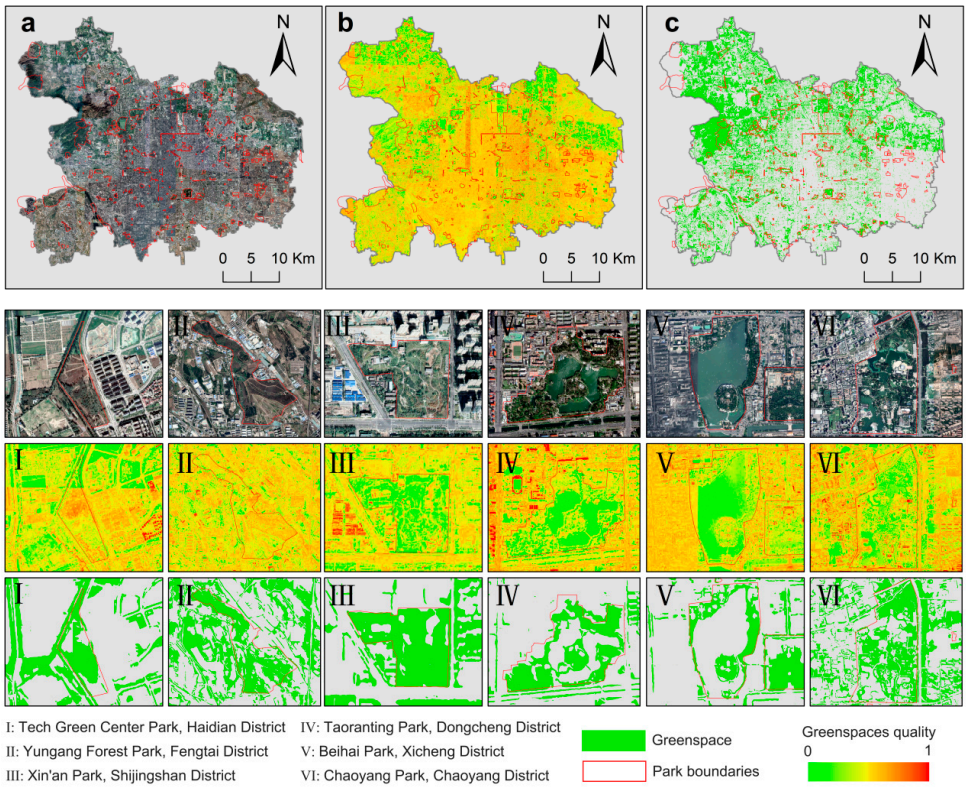


Figure 4. Spatialized referenced remote sensing images depict park patterns, green spaces, and their quality in BBUA. (**a**) Park spatial pattern map; (**b**) green space quality maps; (**c**) spatial distribution of green spaces in BBUA. All subplots display the visual accuracy of information extraction for green spaces in several parks. The remote sensing image base map is from Google Earth. See Equation (1) for the calculation of the green spaces quality indicator.

Spatially, the parks exhibited varying sizes with wide-ranging open areas (Figure 4a), primarily concentrated in the northern region and accompanied by a high EGI (Figure 4b). We reassessed the accuracy of green space data, which yielded a credible accuracy of 87.6%, facilitated by precise 1 m resolution Google Earth remote sensing imagery (Figure A5). We randomly selected six parks and observed their accuracy spatially (Figure 4). Validation results showed that these data are credible and can support further research.

3.2. Exposure Degree of Green Parks

We have presented a map portraying the spatial distribution of green park exposure (Figure 5). It is evident that significant spatial heterogeneity exists, with exposure levels ranging between 0.030 and 0.770 (Figure 5a). Geographically, the exposure performance decreases in concentric circles, from the center outwards. Notably, large-scale forest parks such as Olympic Forest Park, Beigong National Forest Park, and Xishan Park exhibit high levels of exposure (Figure 5a). In terms of quantitative data, the Summer Palace exhibits the highest level of green space exposure at 0.770, followed by Yuyuantan Park and Longtan Lake Park at 0.746 and 0.719, respectively (Figure 5a).

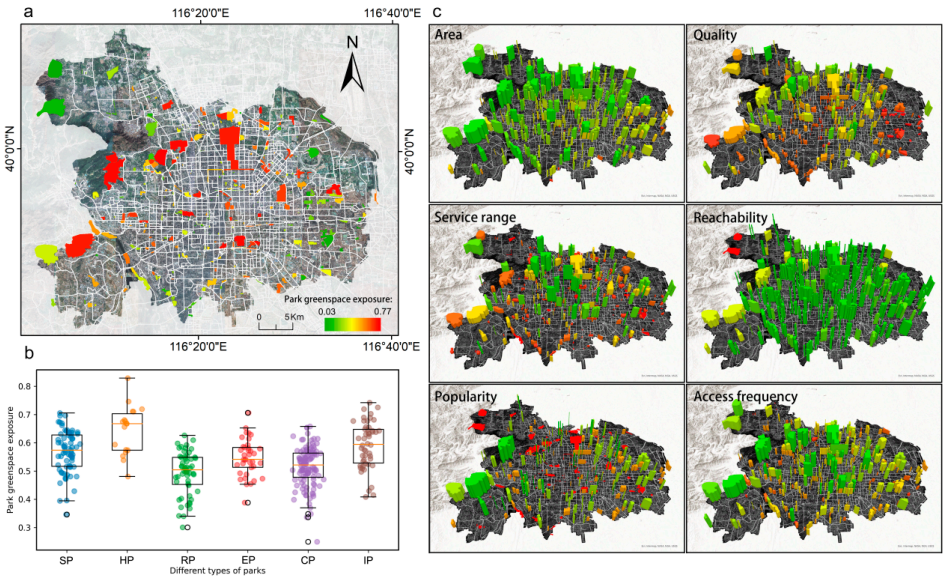


Figure 5. Spatially-explicit map illustrating the exposure performance of the parks' green space. (**a**) Spatially-explicit map of park exposure. (**b**) Exposure degree comparison between parks with different functions. See Figure 1 for abbreviations of park names on the x-axis. (**c**) Performance of different indicators under the exposure framework. In this subplot, the color gradient ranges from red to green, where high green corresponds to better performance.

We observed that six out of ten parks ranked at the top in terms of exposure are historical function parks. In contrast, community and recreational parks generally exhibit a lower level of exposure (Figure 5b). Specifically, from the sample point oscillation amplitude of the box plot in Figure 5, we found significant differences in indicator performance among specialized parks, recreational parks, and community parks, while the exposure gap was relatively smaller among ecological parks (Figure 5b). Under the "3A" assessment criteria, diverse exposure performance was observed among parks. Spatially, the center and southeast of BBUA are accompanied by smaller park areas; in contrast, the north and northwest have larger park areas (Figure 5c). Similarly, the north and northwest of BBUA have better green space quality and significant spatial heterogeneity. Central parks consistently demonstrate better performance in terms of service coverage, accessibility, and frequency of access (Figure 5c).

3.3. Potential Urban Greenways System Patterns

We have identified potential urban greenways to accommodate diverse functions by linking six park functions with transportation swipe card data using the least-cost method, as illustrated in Figure 6. Significant disparities were found in the greenways network in relation to various park functions, providing a range of greenway development options for the distinct needs of residents (Figure 6). All greenways with different functionalities have been planned, spanning a total of 1566.36 km and capable of encompassing 93.88% of the parks (Figure A7). Spatially, park greenways with integrated functions (Figure 6) are densely concentrated in the north and east, with priority given to connecting Chaoyang, Jintian, and Moqiao parks. A total of 15 greenways are in the works, covering 235.15 km (Table 3).

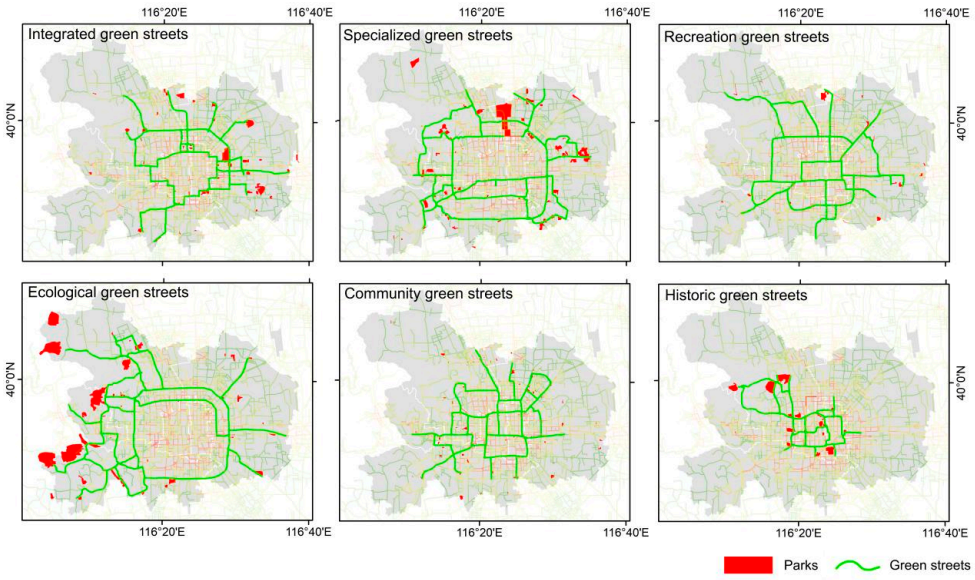


Figure 6. Greenways planning for different park functions. (Using spatial information platforms, we spatially visualized the spatial patterns of different greenways and their spatial distribution differences).

The specialized park greenways aim to connect sports, camping, and music parks primarily located in the outer ring of BBUA's Olympic Park, which spans a total of 318.36 km (Table 3). The recreational park greenways in the central area exhibit radial patterns and have an average length of 17.92 km per greenway (Table 3). The ecological park greenways (Figure 6) are concentrated in the northern and fringe areas, boasting the longest span of greenways, totaling 350.16 km. Conversely, the community park greenways are primarily located in the central area, with the highest number of greenways at 19 and an average span of only 13.08 km (Table 3). The historical park greenways (Figure 6) are also heavily concentrated in central areas, with the shortest span of only 145.22 km. It is worth noting that the average distance of the greenways is only 10.37 km.

We counted the number of recreational passengers at a total of 1167 bus stops on the greenway and compared their travel patterns over the course of a week (Table A2). Our results showed that the planned greenway network can serve between 377,000 and 609,000 passengers per day, accounting for approximately 34.39% to 35.92% of the total recreational volume (Table A2). The number of recreational passengers is particularly high on weekends. Public passengers have greater access to greenways, thereby maximizing the intangible value and benefits of these greenways.

Table 3. The quantitative data related to the various functions of greenway planning were analyzed spatially.

Data Lists	Counts	Length (km)	Mean Length
Integrated parks (IP)	15	235.15	15.68
Specialized parks (SP)	18	318.36	17.69
Ecological parks (EP)	18	350.16	19.45
Community parks (CP)	19	248.60	13.08
Recreation parks (RP)	15	268.87	17.92
Historic parks (HP)	14	145.22	10.37
Total	99	1566.36	15.82

3.4. Obstacle Point Recognition

We further assessed the street-level green view index (GVI) within the network using a street panorama image dataset. Our goal was to identify obstacle points (non-greenways) in the network, providing spatial-level action plans for policymakers to improve the integrity of greenways in BBUA. The results indicated that the average GVI in the study area is 10.78%, with significant spatial variability (Figure 7). Specifically, the central old city area features a mix of streets with varying GVI levels, highlighting the fragmentation of the greenway network. In contrast, connectivity of greenways is higher in peripheral areas, such as Haidian and Shijingshan districts. Notably, low-GVI streets are more prevalent in the southern regions, and main roads and ring roads in BBUA often exhibit poor GVI performance.

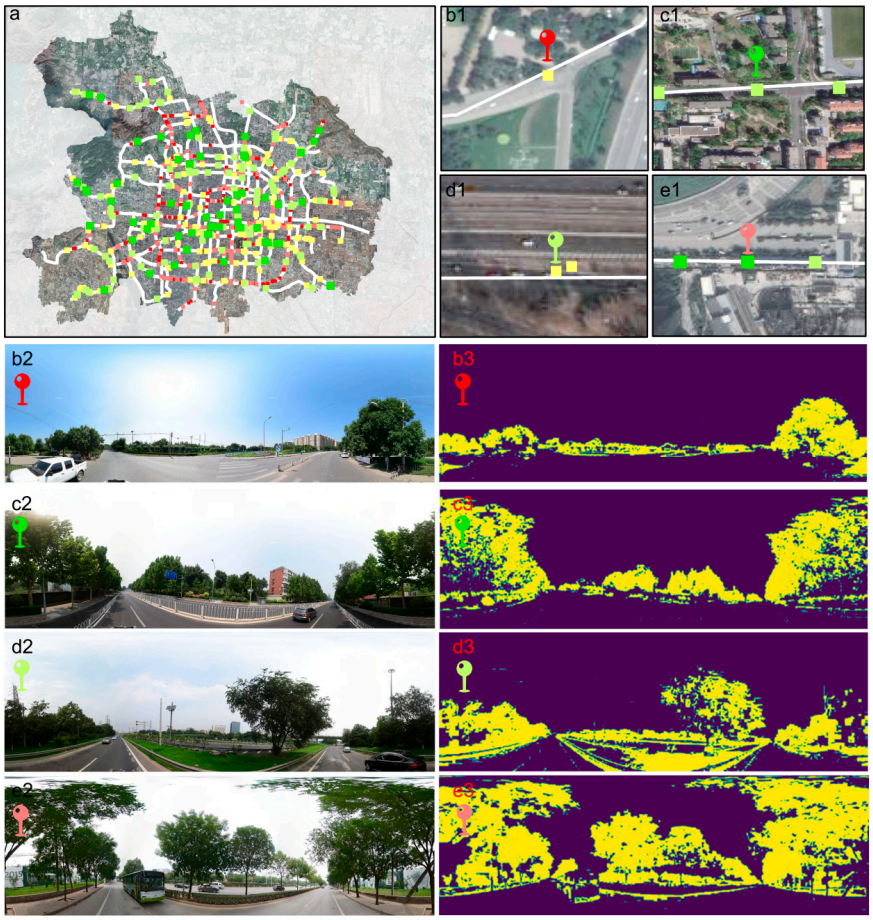


Figure 7. The performance and spatial distribution of the green view index (GVI) in relation to planned greenways are illustrated through panoramic images across four distinct cases. (**a**) Spatially explicit map regarding green view index in planning greenways; (**b1–b3**), (**c1–c3**), (**d1–d3**) and (**e1–e3**) present four different group of panoramic street images and their corresponding green visibility maps.).

4. Discussion

4.1. Implications of Our Study for Urban Greenway Identification

In this study, we employed a user mobility-based framework to identify greenway networks (Figure 2) networks within the BBUA, conceptualizing a comprehensive network blueprint that encompasses 93.88% of urban parks and spans a total of 1566.36 km (Figure 6 and Table 2). Our endeavor sought to interlink each green park in the urban area, forging an effective and accessible network pattern, which amplifies the bus passenger participation (Figure 6). This, in turn, increases the value of ecosystem services of urban greenery, such as stress relief, vision protection, and mental health [3,13]. The greenways engender a symbiotic relationship between ecosystems and well-being [57], fostering a harmonious coexistence between people and nature [58]. Furthermore, this study embraced the concept of versatile greenways, incorporating recreational, ecological, historical, and various other functions to cater to the diverse needs of stakeholders (Figure 6). Multi-functional greenways can energize and personalize cities. In addition, the revitalization and blueprinting of urban greenway are subject to a series of influences, including land valuation dynamics [59], resident preferences [60], and the delicate balance between environmental sustainability and socioeconomic imperatives [61].

We selected Beijing as a case study area because greenway planning is in full swing here. The Beijing government aims to create multi-level, multifaceted greenways that integrate human activities with the natural landscape in Beijing. The 2023–2035 Beijing Greenway System Special Plan proposes to build greenways that synergistically include elements of commerce, ingenuity, and art [62]. In addition, greenway policymakers have attempted to rely on greenway networks to mitigate inequities in human exposure to green space [1]. Greenway construction is also an integral part of an ecological and sustainable city [63]. The greenway network we planned can be considered to maximize passenger access to street greenery. The results showed that although the total length of the network is only 1566.36 km, it can be accessed by approximately 33.39–35.92% of bus passengers (Table A2). The on-street system provides a green and low-carbon mode of travel, and passengers are more likely to interact with the outside scenery [53]. In addition, Beijing's greenway system, planned to span more than 5000 km, aims to connect urban and rural areas. The extension of greenways in urban fringe zones augments connectivity [64] among wildlands, national reserves, and forested areas, thereby enhancing solutions for nature-based ecosystems [65], biodiversity [26], and human well-being [57]. This extensive network has also has the potential to alleviate the urban–rural divide and reduce inequalities in green space access [62]. Our results indicate that some greenways, such as the circular arterial, are included in Beijing greenway planning practices. However, greenways in central built-up areas are often overlooked by policymakers (Figure 7).

We described this framework as a multi-source big data-driven framework, which contains big data on transit trips and user reviews (Figure 2). User-based big data can capture stakeholders' intuitive experiences of greenways [27]. Here, we consider the recreational mobility patterns of more than ten million people from bus transportation datasets, and assesses the exposure level of park green spaces based on the integration of social media and geospatial data (Figure 2). In contrast to conventional methodologies, the utilization of big data in greenways planning offers a robust approach, underpinned by extensive samples of human behavioral patterns (Figure 3). Our framework endeavors to yield systematic outcomes while prioritizing the optimization of human well-being (Figure 6).

Street vegetation has been widely acknowledged to amplify leisure and verdant physical engagements, and augment the ecological integrity of urban surroundings [66]. As evident from our results, based on Baidu panoramic imagery, persisting issues such as greenway disruptions and congestion remain prevalent (Figure 7a). Beijing's urban blueprint laid out by the Beijing municipal authorities, emphasizes the imperative of factoring in greenway connectivity and coherence throughout the urban rejuvenation and shantytown reformation endeavors (https://www.beijing.gov.cn/). Serving as the vanguard city in the nation's drive for building reduction, Beijing has downsized urban and rural construction land by a stagger-

ing 110 km^2 as of June 2023 (https://yllhj.beijing.gov.cn), as part of its green development and carbon neutrality aspirations. In addition, we also emphasize that images of the city, such as street panoramas, surveillance cameras, and tourist-sharing images, will play an increasingly important role in urban greenway planning.

4.2. Limitations and Uncertainties

Here, we initially planned multifunctional greenways leveraging multi-source big data, including geographic information data, remote sensing data, and review data (Table 1). Although the ample sample size provides scientific and credible research results, this work still faces several challenges. The redundancy and representativeness of indicators within the green space exposure assessment framework need to be examined to ensure the reliability of the "3A" framework. In terms of data, our focus solely on greenway planning along bus routes limits the potential for greening non-bus routes, such as private and internet cars. We also did not include non-green parks in the scope of our study, such as car parks and commercial parks. We have given greenways a narrower definition that excludes walking and forest greenways. Filtering recreational travel patterns from traffic travel data remains challenging due to the unpredictable travel characteristics of some passengers caused by work. Additionally, studies have shown that GVI extraction based on deep learning algorithms and convolutional neural networks is more convincing [67]. However, this study only used a threshold model to consider time efficiency (Figure 7).

Spatially, our study area was solely focused on the urban area of Beijing, without considering the wildland–urban interface [68], due to the spatial constraints of geographic information data. Cross-regional metacoupling processes based on tourist mobility were not further considered in this study [69]. Furthermore, greenways under sustainable cities encompass various aspects including low-carbon, water permeability [70], stormwater management, and community adaptability [71]. The assessment of greenway performance still requires field surveys to obtain credible data based on stakeholder interests [39]. These challenges need to be addressed in future research; nonetheless, we offer a new perspective on planning greenways in urban areas.

5. Conclusions

Here, we introduced a greenway identification framework, which incorporates park green space exposure and user-based bus transportation flows. Our results showed that the greenways network planned in BBUA spans 1566.36 km, covering 93.88% of the parks and encompassing six functions. This network can serve 34.39% to 35.92% of bus recreation passengers, with this ratio tending to be higher on weekends. However, we found that the greenway network is unconnected, especially in the central built-up areas and the southern trunk road. These obstacle points should receive focused attention from urban planners to build robust and highly connected greenways. We presented an efficient user-based framework for greenway planning in urban areas, which provides a new perspective on potential urban greenway identification.

Author Contributions: T.L.: Conceptualization, Methodology, Software, Visualization, Writing—original draft. L.Y.: Conceptualization, Supervision, Funding acquisition, Writing—review and editing. X.C.: Funding acquisition, Methodology, Writing—review and editing. Y.C. (Yunmiao Chen): Data curation. X.L. (Xiaomeng Li): Data curation. X.L. (Xinyi Liu): Data curation. Y.C. (Yue Cao): Review and editing. F.Z.: Methodology. C.Z.: Review and editing. P.G.: Review and editing. All authors have read and agreed to the published version of the manuscript.

Funding: This research was supported by the National Key R&D Program of China (2022YFE0209400) and the Tsinghua University Initiative Scientific Research Programs (20223080017); China Postdoctoral Science Foundation (2022M711755).

Informed Consent Statement: All participants involved in this study provided their informed consent.

Data Availability Statement: The POI and AOI data related to Beijing's parks, the road network with topological relationships, street panoramic images involved in this study, and all Python codes are

available at 10.6084/m9.figshare.25358113. The bus traffic data for the week of February 13th to 19th, 2023 in Beijing and other data used in this paper are available from the corresponding author upon reasonable request.

Conflicts of Interest: The authors declare that they have no known competing financial interests or personal relationships that would have influenced the work reported in this paper.

Appendix A. Accessibility Analysis of BBUA

The accessibility of 331 parks in BBUA is an important data input for the "Availability–Accessibility–Adaptability" (3A) assessment framework. Park accessibility can reflect the frequency of human movement to green parks, thereby revealing the level of community exposure to park green spaces. We aim to reflect accessibility performance by studying the connectivity costs of multiple origins and destinations in the study area's transportation network. Therefore, this study adopts an origin–destination (OD) cost matrix model, which can be fully implemented in ArcMap (https://arcgis.com).

The workflow of this study began with the retrieval of 2023 road data for Beijing from the OpenStreetMap platform (https://openstreetmap.org/). This dataset encompasses roads of various grades, ranging from highways to sidewalks, with the vector road data existing in a non-topological state. To construct a multi-grade road network structure, we extracted three levels of road networks based on road width and driving speed criteria (https://www.mot.gov.cn/). The first-level road network comprises highways and national roads, the second-level road network includes expressways and main roads, while the third-level road network encompasses motor vehicle streets and similar thoroughfares. Subsequently, to establish the topological relationships of the road network (Figure A1), we conducted a series of network repair procedures, including road buffering (10 m), extension, linking, and segmentation, all of which are accessible within the ArcMap editor tools.

We established a multi-level road network for the study area with topological relationships (Figure A1), where each road node is connected and traversable. Following the creation of the feature dataset, we manually examined the usability of the road network once more and retained the topologically connected road network database as a backup (Figure A1). We assigned speed limits to the roads: first-level roads at 70 km/h, second-level roads at 50 km/h, and third-level roads at 30 km/h (https://www.mot.gov.cn/). Finally, we obtained the accessibility raster dataset based on the newly created origin–destination (OD) cost matrix, and this result was spatially visualized in Figure A1.

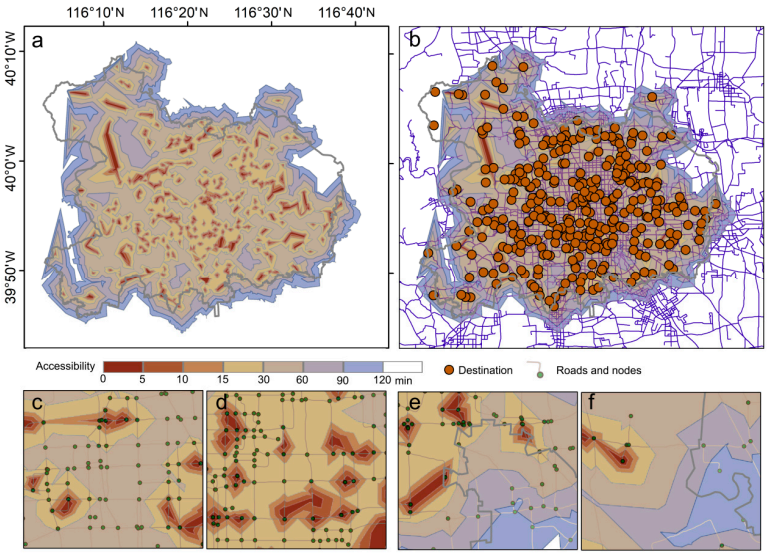


Figure A1. The accessibility and topological patterns of BBUA. (**a**) Spatial visualization of accessibility in BBUA. (**b**) Road network patterns and spatial distribution of parks. (**c**–**f**). are examples of road network topological relationships.)

Appendix B. Calculating Green View Index Based on Street Panoramic Images

The acquisition of street view panoramic images was conducted utilizing the street view imagery (SVI) from the Baidu Street View service. To ensure a comprehensive coverage while preventing data redundancy, sampling points were systematically generated along the road network at intervals of 50 m. These intervals were determined based on the road topology information provided by OpenStreetMap (OSM). For the extraction and retrieval of the images, a Python script was developed leveraging the Baidu Street Map API. The script systematically requested street view images corresponding to the predefined sampling points. Each request to the Baidu Street View service API followed the format: http://api.map.com/panorama/v2?ak=YOUR_KEY&width=WIDTH&height=HEIGHT&location=LON,LAT (accessed on 25 September 2024).

Where YOUR_KEY is the API key provided to authorized users, and WIDTH, HEIGHT, LON, and LAT were parameters set according to the requirements of our analysis. Through this automated process, we successfully acquired a total of xx street view images, which were subsequently utilized for detailed streetscape analysis. Here, we constructed a decision tree to evaluate the green view ratio indicators of street panoramas (Figure A2).

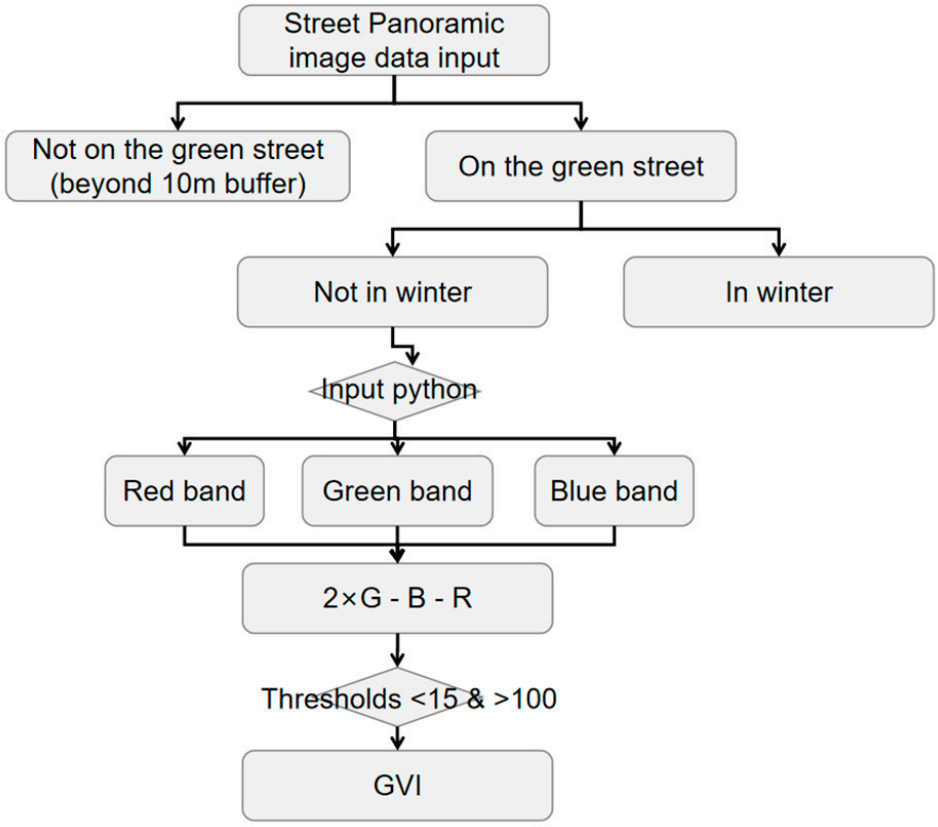


Figure A2. Decision tree for calculating GVI. (In this study, we employed an empirical model to assess the green area and its proportion in street panorama RGB images. Compared to image recognition-related deep learning algorithms, such as semantic segmentation and convolutional neural networks, the advantage of this algorithm lies in its ability to provide quick and efficient results. We calculated the GVI for each image and used a threshold to determine the green area on the photo. After multiple iterations, the optimal threshold for this model was determined to be between 15% and 100%).

Appendix C. Appendix Figures

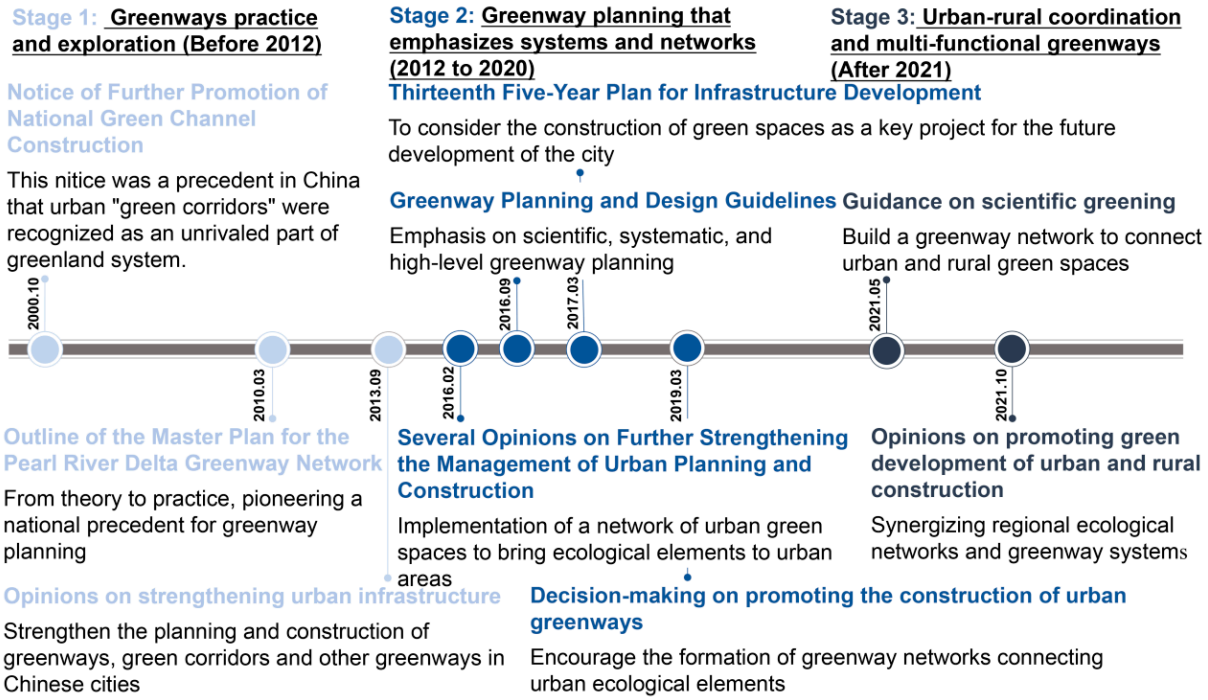


Figure A3. The timeline evolution of China's greenway planning policies: a three-stage development. (We reviewed the greenway planning policies issued by the Chinese government and classified them into three stages, each with unique greenway themes and objectives. As time passed, there was a growing emphasis on systemic, organizational, and integrated approaches.).

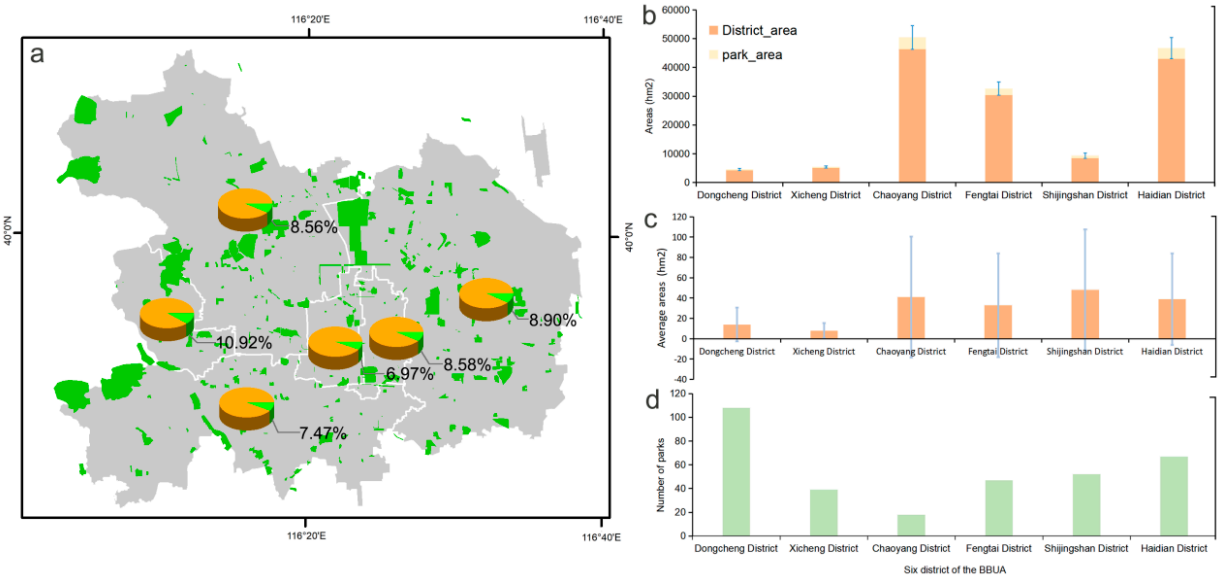


Figure A4. Essential quantitative green park information about sub-administrative in BBUA. (We calculated the green space area related to parks in each sub-administrative area of BBUA, which is crucial for implementing green space planning and construction projects based on green equity and accessibility. (**a**) The spatial pattern and percentage of park space in six districts. (**b**) Total area of the park. (**c**) Average areas of parks. (**d**) The number of parks in six districts.).

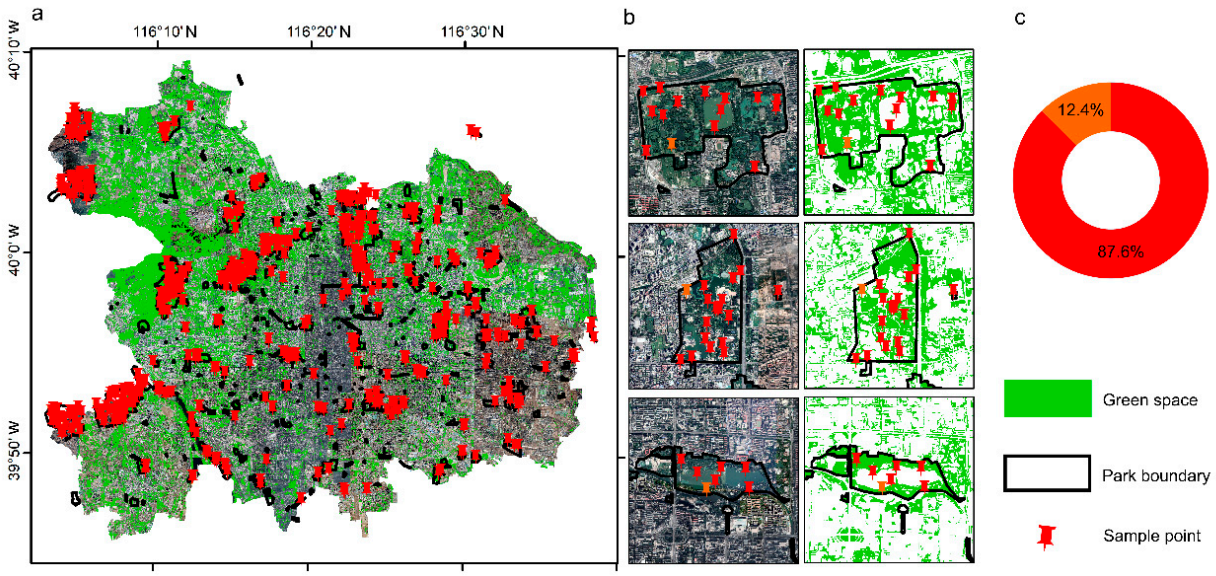


Figure A5. The spatial distribution pattern and three case studies of the accuracy assessment of park green lands in BBUA. (Here, we used a random sample point model to calculate the accuracy of park green spaces. We randomly generated 500 sample points within the parks and compared them with Google Earth images. The accuracy of manually marked park green lands was assigned a value of 1, resulting in a final accuracy of 87.6%. The reliability of the accuracy of our park green space data supports our next research.).

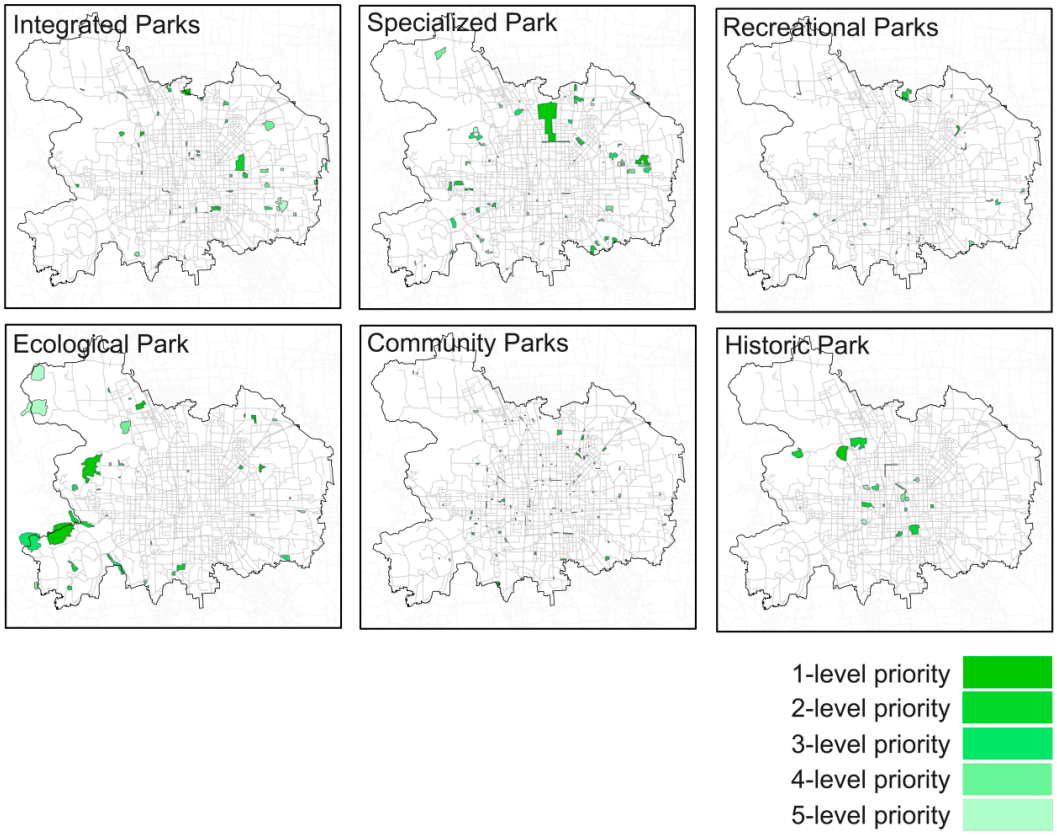


Figure A6. Planning the priority of greenway carrier. (In this study, we divided the exposure of park green spaces into five levels using a natural break point method. The first two levels are used as carriers for linking the greenway network.).

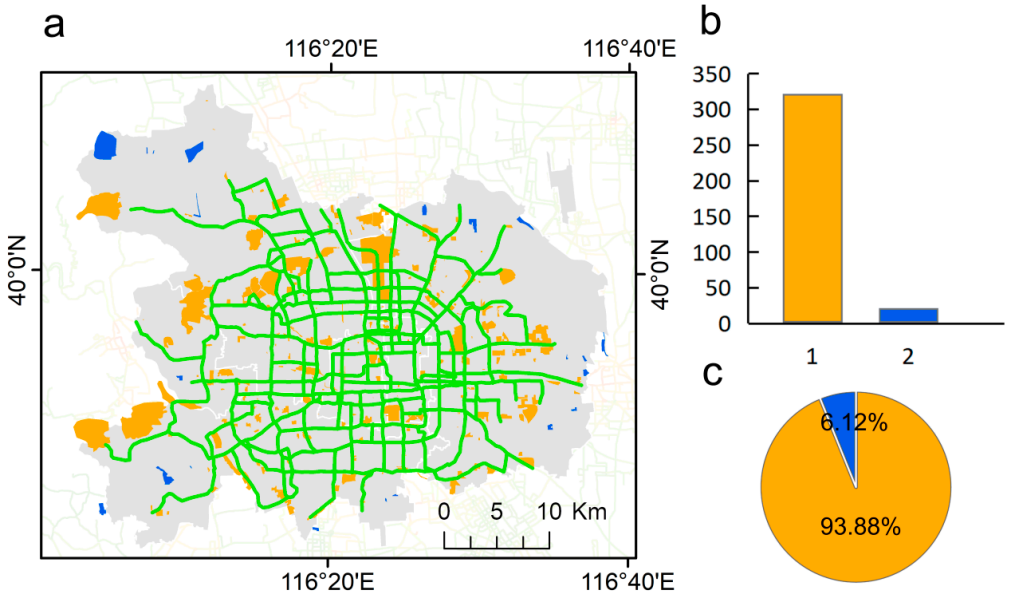


Figure A7. Planning the green streets system involving accessible and inaccessible parks. (Through overlay analysis and walk buffs based on a 15-min catchment area, we assessed the accessibility of green parks reached by planned greenways. (**a**). Spatially-explicit map concerning accessible and inaccessible parks. (**b**). Number of accessible and inaccessible parks. (**c**). Percentage of accessible and inaccessible parks).

Table A1. Service area corresponds to six different types of parks. (We reference the official national standard, namely the Basic Requirements of the Park Service (https://openstd.samr.gov.cn), to determine the areas of park service.).

Parks	Service Areas/m
Historic park	2000
Community parks	500
Ecological park	800
Recreational parks	300
Specialized park	1000
Integrated parks	1500

Table A2. Number and share of recreational passenger at bus stops corresponding to the green street network. (/per).

Parks	Monday	Tuesday	Wednesday	Thursday	Friday	Saturday	Sunday
Historic park (/per)	28,970	44,730	44,662	45,518	42,970	32,546	39,184
Community parks (/per)	69,391	108,474	108,168	111,152	105,762	78,040	94,156
Ecological park (/per)	58,958	94,880	94,952	96,324	92,978	69,532	78,088
Recreational parks (/per)	83,620	134,642	133,910	136,318	129,764	95,488	113,796
Specialized park (/per)	60,306	96,416	95,162	97,642	93,168	69,550	81,846
Integrated parks (/per)	75,428	118,498	119,712	121,824	117,430	85,334	101,098
Total (/per)	1,048,575	1,671,566	1,671,084	1,697,340	1,654,358	1,251,630	1,422,150
Historic park (%)	2.76%	2.68%	2.67%	2.68%	2.60%	2.60%	2.76%
Community parks (%)	6.62%	6.49%	6.47%	6.55%	6.39%	6.24%	6.62%
Ecological park (%)	5.62%	5.68%	5.68%	5.67%	5.62%	5.56%	5.49%
Recreational parks (%)	7.97%	8.05%	8.01%	8.03%	7.84%	7.63%	8.00%
Specialized park (%)	5.75%	5.77%	5.69%	5.75%	5.63%	5.56%	5.76%
Integrated parks (%)	7.19%	7.09%	7.16%	7.18%	7.10%	6.82%	7.11%
Total (%)	1	1	1	1	1	1	1

References

1. Leng, S.; Sun, R.; Yang, X.; Chen, L. Global Inequities in Population Exposure to Urban Greenspaces Increased amidst Tree and Nontree Vegetation Cover Expansion. *Commun. Earth Environ.* **2023**, *4*, 464. [CrossRef]
2. Liu, T.; Yu, L.; Liu, J.; Xu, Z.; Chen, X.; Wu, H.; Zheng, S.; Zhao, Q.; Gong, P. Unveiling Interprovincial Geographic Patterns of 5A-Level Tourism Cultural Ecosystem Service Flows and Tourist Preferences in China's Metacoupled Systems. *Appl. Geogr.* **2024**, *172*, 103432. [CrossRef]
3. Mu, B.; Liu, C.; Tian, G.; Xu, Y.; Zhang, Y.; Mayer, A.L.; Lv, R.; He, R.; Kim, G. Conceptual Planning of Urban–Rural Green Space from a Multidimensional Perspective: A Case Study of Zhengzhou, China. *Sustainability* **2020**, *12*, 2863. [CrossRef]
4. Elmqvist, T.; Andersson, E.; Frantzeskaki, N.; McPhearson, T.; Olsson, P.; Gaffney, O.; Takeuchi, K.; Folke, C. Sustainability and Resilience for Transformation in the Urban Century. *Nat. Sustain.* **2019**, *2*, 267–273. [CrossRef]
5. Li, F.; Liu, X.; Zhang, X.; Zhao, D.; Liu, H.; Zhou, C.; Wang, R. Urban Ecological Infrastructure: An Integrated Network for Ecosystem Services and Sustainable Urban Systems. *J. Clean. Prod.* **2017**, *163*, S12–S18. [CrossRef]
6. Erlwein, S.; Zölch, T.; Pauleit, S. Regulating the Microclimate with Urban Green in Densifiying Cities: Joint Assessment on Two Scales. *Build. Environ.* **2021**, *205*, 108233. [CrossRef]
7. Zimmermann, E.; Bracalenti, L.; Piacentini, R.; Inostroza, L. Urban Flood Risk Reduction by Increasing Green Areas for Adaptation to Climate Change. *Procedia Eng.* **2016**, *161*, 2241–2246. [CrossRef]
8. Sun, M.; Yang, R.; Li, X.; Zhang, L.; Liu, Q. Designing a Path for the Sustainable Development of Key Ecological Function Zones: A Case Study of Southwest China. *Glob. Ecol. Conserv.* **2021**, *31*, e01840. [CrossRef]
9. Dybala, K.E.; Matzek, V.; Gardali, T.; Seavy, N.E. Carbon Sequestration in Riparian Forests: A Global Synthesis and Meta-analysis. *Glob. Change Biol.* **2019**, *25*, 57–67. [CrossRef]
10. Filazzola, A.; Shrestha, N.; MacIvor, J.S. The Contribution of Constructed Green Infrastructure to Urban Biodiversity: A Synthesis and Meta-analysis. *J. Appl. Ecol.* **2019**, *56*, 2131–2143. [CrossRef]
11. Potter, J.D.; Brooks, C.; Donovan, G.; Cunningham, C.; Douwes, J. A Perspective on Green, Blue, and Grey Spaces, Biodiversity, Microbiota, and Human Health. *Sci. Total Environ.* **2023**, *892*, 164772. [CrossRef] [PubMed]
12. Ahern, J. Greenways as a Planning Strategy. *Landsc. Urban Plan.* **1995**, *33*, 131–155. [CrossRef]
13. Cleary, A.; Roiko, A.; Burton, N.W.; Fielding, K.S.; Murray, Z.; Turrell, G. Changes in Perceptions of Urban Green Space Are Related to Changes in Psychological Well-Being: Cross-Sectional and Longitudinal Study of Mid-Aged Urban Residents. *Health Place* **2019**, *59*, 102201. [CrossRef] [PubMed]
14. Jabbar, M.; Yusoff, M.M.; Shafie, A. Assessing the Role of Urban Green Spaces for Human Well-Being: A Systematic Review. *GeoJournal* **2022**, *87*, 4405–4423. [CrossRef]
15. Bryant, M.M. Urban Landscape Conservation and the Role of Ecological Greenways at Local and Metropolitan Scales. *Landsc. Urban Plan.* **2006**, *76*, 23–44. [CrossRef]
16. Liangjun, H.; Yunhua, A. Study on Urban Greenway Improvement Strategies from the Perspective of Landscape Justice. *J. Landsc. Res.* **2021**, *13*, 1–10. [CrossRef]
17. Balta, M.Ö.; Yenil, H.Ü. Multi Criteria Decision Making Methods for Urban Greenway: The Case of Aksaray, Turkey. *Land Use Policy* **2019**, *89*, 104224. [CrossRef]
18. Lu, J.; Wu, X. Research on Urban Greenway Alignment Selection Based on Multisource Data. *Sustainability* **2022**, *14*, 12382. [CrossRef]
19. Tang, Z.; Ye, Y.; Jiang, Z.; Fu, C.; Huang, R.; Yao, D. A Data-Informed Analytical Approach to Human-Scale Greenway Planning: Integrating Multi-Sourced Urban Data with Machine Learning Algorithms. *Urban For. Urban Green.* **2020**, *56*, 126871. [CrossRef]
20. Xu, H.; Plieninger, T.; Primdahl, J. A Systematic Comparison of Cultural and Ecological Landscape Corridors in Europe. *Land* **2019**, *8*, 41. [CrossRef]
21. Zhou, Y.; Varquez, A.C.G.; Kanda, M. High-Resolution Global Urban Growth Projection Based on Multiple Applications of the SLEUTH Urban Growth Model. *Sci. Data* **2019**, *6*, 34. [CrossRef] [PubMed]
22. Shoshany, M.; Shapira, A.; Nir-Goldenberg, S.; De Paola, P. Progression of Greenway Corridors Through Conflict: Cellular Automata Simulation and AHP Evaluation. *Environ. Model. Assess.* **2023**, *28*, 519–533. [CrossRef]
23. Lopes, I.J.C.; Biondi, D.; Corte, A.P.D.; Reis, A.R.N.; Oliveira, T.G.S. A Methodological Framework to Create an Urban Greenway Network Promoting Avian Connectivity: A Case Study of Curitiba City. *Urban For. Urban Green.* **2023**, *87*, 128050. [CrossRef]
24. Gomes, G.D.; Batista, D.L.; Silva, P.G. Changing Scales: Greenways from Region to Place—The Case of The Algarve, Portugal. In Proceedings of the Fábos Conference on Landscape and Greenway Planning, Budapest, Hungary, 30 June–3 July 2022; University of Massachusetts Amherst Libraries: St. Amherst, MA, USA, 2022; Volume 7, p. 1. [CrossRef]
25. Ding, C.; Song, Y.; Qiao, X.; Zhang, Y.; Yu, B.; Zhang, X. Integrating Land Use and Greenway Network for Metro Station Area Transit-Oriented Development. *Transp. Res. Part D Transp. Environ.* **2022**, *113*, 103539. [CrossRef]
26. Carlier, J.; Moran, J. Landscape Typology and Ecological Connectivity Assessment to Inform Greenway Design. *Sci. Total Environ.* **2019**, *651*, 3241–3252. [CrossRef]
27. Jia, J.; Zhang, X. A Human-Scale Investigation into Economic Benefits of Urban Green and Blue Infrastructure Based on Big Data and Machine Learning: A Case Study of Wuhan. *J. Clean. Prod.* **2021**, *316*, 128321. [CrossRef]
28. Frank, L.D.; Hong, A.; Ngo, V.D. Build It and They Will Cycle: Causal Evidence from the Downtown Vancouver Comox Greenway. *Transp. Policy* **2021**, *105*, 1–11. [CrossRef]

29. Pang, J.; Huang, J.; Yang, X.; Wang, Z.; Yu, H.; Huang, Q.; Yin, B. Discovering Fine-Grained Spatial Pattern from Taxi Trips: Where Point Process Meets Matrix Decomposition and Factorization. *IEEE Trans. Intell. Transport. Syst.* **2018**, *19*, 3208–3219. [CrossRef]
30. Liu, Y.; Lu, A.; Yang, W.; Tian, Z. Investigating Factors Influencing Park Visit Flows and Duration Using Mobile Phone Signaling Data. *Urban For. Urban Green.* **2023**, *85*, 127952. [CrossRef]
31. Cheng, X.; Van Damme, S.; Uyttenhove, P. A Review of Empirical Studies of Cultural Ecosystem Services in Urban Green Infrastructure. *J. Environ. Manag.* **2021**, *293*, 112895. [CrossRef]
32. Larson, L.R.; Keith, S.J.; Fernandez, M.; Hallo, J.C.; Shafer, C.S.; Jennings, V. Ecosystem Services and Urban Greenways: What's the Public's Perspective? *Ecosyst. Serv.* **2016**, *22*, 111–116. [CrossRef]
33. Chang, P.-J. Effects of the Built and Social Features of Urban Greenways on the Outdoor Activity of Older Adults. *Landsc. Urban Plan.* **2020**, *204*, 103929. [CrossRef]
34. Shahtahmassebi, A.R.; Li, C.; Fan, Y.; Wu, Y.; Lin, Y.; Gan, M.; Wang, K.; Malik, A.; Blackburn, G.A. Remote Sensing of Urban Green Spaces: A Review. *Urban For. Urban Green.* **2021**, *57*, 126946. [CrossRef]
35. Kumakoshi, Y.; Chan, S.Y.; Koizumi, H.; Li, X.; Yoshimura, Y. Standardized Green View Index and Quantification of Different Metrics of Urban Green Vegetation. *Sustainability* **2020**, *12*, 7434. [CrossRef]
36. Li, X.; Zhang, C.; Li, W.; Ricard, R.; Meng, Q.; Zhang, W. Assessing Street-Level Urban Greenery Using Google Street View and a Modified Green View Index. *Urban For. Urban Green.* **2015**, *14*, 675–685. [CrossRef]
37. Yang, J.; Zhao, L.; Mcbride, J.; Gong, P. Can You See Green? Assessing the Visibility of Urban Forests in Cities. *Landsc. Urban Plan.* **2009**, *91*, 97–104. [CrossRef]
38. Harden, S.R.; Schuurman, N.; Larson, H.; Walker, B.B. The Utility of Street View Imagery in Environmental Audits for Runnability. *Appl. Geogr.* **2024**, *162*, 103167. [CrossRef]
39. Horte, O.; Eisenman, T. Urban Greenways: A Systematic Review and Typology. *Land* **2020**, *9*, 40. [CrossRef]
40. Hou, L.; Liu, T.; Wang, J.; Chen, X.; Du, Z.; Xu, S.; Yu, L. Land Disturbance Tempo-Spatial Dynamics in Mountainous Urban Agglomeration and Its Driving Forces: A Case Study of West Sichuan Urban Agglomeration, China. *Ecol. Indic.* **2023**, *154*, 110569. [CrossRef]
41. Li, G.; Li, F. Urban Sprawl in China: Differences and Socioeconomic Drivers. *Sci. Total Environ.* **2019**, *673*, 367–377. [CrossRef]
42. Du, Z.; Yu, L.; Chen, X.; Li, X.; Peng, D.; Zheng, S.; Hao, P.; Yang, J.; Guo, H.; Gong, P. An Operational Assessment Framework for Near Real-Time Cropland Dynamics: Toward Sustainable Cropland Use in Mid-Spine Belt of Beautiful China. *J. Remote Sens.* **2023**, *3*, 0065. [CrossRef]
43. Zhang, Y.; Shen, W.; Li, M.; Lv, Y. Assessing Spatio-Temporal Changes in Forest Cover and Fragmentation under Urban Expansion in Nanjing, Eastern China, from Long-Term Landsat Observations (1987–2017). *Appl. Geogr.* **2020**, *117*, 102190. [CrossRef]
44. Tian, L.; Li, Y.; Lu, J.; Wang, J. Review on Urban Heat Island in China: Methods, Its Impact on Buildings Energy Demand and Mitigation Strategies. *Sustainability* **2021**, *13*, 762. [CrossRef]
45. Cao, J.; Grigor'yan, A.; Liu, L. Hardy's Inequality and Green Function on Metric Measure Spaces. *J. Funct. Anal.* **2021**, *281*, 109020. [CrossRef]
46. Wu, J.; Qian, M.; Cao, Y. Research on the Influence Mechanism and Optimisation of Urban Greenway Network Use Pattern Based on Multi-Source Data—A Case Study of Guangzhou, China. In Proceedings of the Fábos Conference on Landscape and Greenway Planning, Budapest, Hungary, 30 June–3 July 2022; University of Massachusetts Amherst Libraries: St. Amherst, MA, USA, 2022; Volume 7, p. 1. [CrossRef]
47. Teng, M.; Wu, C.; Zhou, Z.; Lord, E.; Zheng, Z. Multipurpose Greenway Planning for Changing Cities: A Framework Integrating Priorities and a Least-Cost Path Model. *Landsc. Urban Plan* **2011**, *103*, 1–14. [CrossRef]
48. Keith, S.J.; Larson, L.R.; Shafer, C.S.; Hallo, J.C.; Fernandez, M. Greenway Use and Preferences in Diverse Urban Communities: Implications for Trail Design and Management. *Landsc. Urban Plan.* **2018**, *172*, 47–59. [CrossRef]
49. Wu, J.; Yu, Z.; Wei, Y.D.; Yang, L. Changing Distribution of Migrant Population and Its Influencing Factors in Urban China: Economic Transition, Public Policy, and Amenities. *Habitat Int.* **2019**, *94*, 102063. [CrossRef]
50. Shi, Q.; Liu, M.; Marinoni, A.; Liu, X. UGS-1m: Fine-Grained Urban Green Space Mapping of 31 Major Cities in China Based on the Deep Learning Framework. *Earth Syst. Sci. Data* **2023**, *15*, 555–577. [CrossRef]
51. Yu, Z.; Ma, W.; Hu, S.; Yao, X.; Yang, G.; Yu, Z.; Jiang, B. A Simple but Actionable Metric for Assessing Inequity in Resident Greenspace Exposure. *Ecol. Indic.* **2023**, *153*, 110423. [CrossRef]
52. Cao, M.; Yao, H.; Li, J. Accessibility-Based Equity Assessment of Urban Parks in Beijing. *J. Urban Plann. Dev.* **2021**, *147*, 05021018. [CrossRef]
53. Balbi, M.; Croci, S.; Petit, E.J.; Butet, A.; Georges, R.; Madec, L.; Caudal, J.-P.; Ernoult, A. Least-cost Path Analysis for Urban Greenways Planning: A Test with Moths and Birds across Two Habitats and Two Cities. *J. Appl. Ecol.* **2020**, *24*, 632–643. [CrossRef]
54. Pena, S.B.; Abreu, M.M.; Teles, R.; Espírito-Santo, M.D. A Methodology for Creating Greenways through Multidisciplinary Sustainable Landscape Planning. *J. Environ. Manag.* **2010**, *91*, 970–983. [CrossRef]
55. Zeng, L.; Lu, J.; Li, W.; Li, Y. A Fast Approach for Large-Scale Sky View Factor Estimation Using Street View Images. *Build. Environ.* **2018**, *135*, 74–84. [CrossRef]
56. Wu, C.; Ye, Y.; Gao, F.; Ye, X. Using Street View Images to Examine the Association between Human Perceptions of Locale and Urban Vitality in Shenzhen, China. *Sustain. Cities Soc.* **2023**, *88*, 104291. [CrossRef]

57. Chang, P.-J.; Tsou, C.-W.; Li, Y.-S. Urban-Greenway Factors' Influence on Older Adults' Psychological Well-Being: A Case Study of Taichung, Taiwan. *Urban For. Urban Green.* **2020**, *49*, 126606. [CrossRef]
58. Kent, R.L.; Elliott, C.L. Scenic Routes Linking and Protecting Natural and Cultural Landscape Features: A Greenway Skeleton. *Landsc. Urban Plan.* **1995**, *33*, 341–355. [CrossRef]
59. Xie, X.; Dries, L.; Heijman, W.; Zhang, A. Land Value Creation and Benefit Distribution in the Process of Rural-Urban Land Conversion: A Case Study in Wuhan City, China. *Habitat Int.* **2021**, *109*, 102335. [CrossRef]
60. Tu, G.; Abildtrup, J.; Garcia, S. Preferences for Urban Green Spaces and Peri-Urban Forests: An Analysis of Stated Residential Choices. *Landsc. Urban Plan.* **2016**, *148*, 120–131. [CrossRef]
61. Lu, Y. Using Google Street View to Investigate the Association between Street Greenery and Physical Activity. *Landsc. Urban Plan.* **2019**, *191*, 103435. [CrossRef]
62. BMCPNR Beijing Greenway System Special Plan (2023–2035). 2024. Available online: https://ghzrzyw.beijing.gov.cn/zhengwuxinxi/ghcg/zxgh/202404/t20240428_3643306.html (accessed on 25 September 2024).
63. Li, X.; Wang, X.; Jiang, X.; Han, J.; Wang, Z.; Wu, D.; Lin, Q.; Li, L.; Zhang, S.; Dong, Y. Prediction of Riverside Greenway Landscape Aesthetic Quality of Urban Canalized Rivers Using Environmental Modeling. *J. Clean. Prod.* **2022**, *367*, 133066. [CrossRef]
64. Sarkar, C.; Webster, C.; Pryor, M.; Tang, D.; Melbourne, S.; Zhang, X.; Jianzheng, L. Exploring Associations between Urban Green, Street Design and Walking: Results from the Greater London Boroughs. *Landsc. Urban Plan.* **2015**, *143*, 112–125. [CrossRef]
65. Préau, C.; Tournebize, J.; Lenormand, M.; Alleaume, S.; Boussada, V.G.; Luque, S. Habitat Connectivity in Agricultural Landscapes Improving Multi-Functionality of Constructed Wetlands as Nature-Based Solutions. *Ecol. Eng.* **2022**, *182*, 106725. [CrossRef]
66. Ordóñez, C.; Duinker, P.N. Ecological Integrity in Urban Forests. *Urban Ecosyst.* **2012**, *15*, 863–877. [CrossRef]
67. Campbell, A.; Both, A.; Sun, Q. Detecting and Mapping Traffic Signs from Google Street View Images Using Deep Learning and GIS. *Comput. Environ. Urban Syst.* **2019**, *77*, 101350. [CrossRef]
68. Chen, B.; Wu, S.; Jin, Y.; Song, Y.; Wu, C.; Venevsky, S.; Xu, B.; Webster, C.; Gong, P. Wildfire Risk for Global Wildland–Urban Interface Areas. *Nat. Sustain.* **2024**, *7*, 474–484. [CrossRef]
69. Liu, J. Integration across a Metacoupled World. *Ecol. Soc.* **2017**, *22*, 29. [CrossRef]
70. Barber, A.; Haase, D.; Wolff, M. Permeability of the City—Physical Barriers of and in Urban Green Spaces in the City of Halle, Germany. *Ecol. Indic.* **2021**, *125*, 107555. [CrossRef]
71. Ni'mah, N.M.; Lenonb, S. Urban Greenspace for Resilient City in the Future: Case Study of Yogyakarta City. *IOP Conf. Ser. Earth Environ. Sci.* **2017**, *70*, 012058. [CrossRef]

Disclaimer/Publisher's Note: The statements, opinions and data contained in all publications are solely those of the individual author(s) and contributor(s) and not of MDPI and/or the editor(s). MDPI and/or the editor(s) disclaim responsibility for any injury to people or property resulting from any ideas, methods, instructions or products referred to in the content.